

Jeffrey R. French<sup>†</sup>, Timothy L. Crawford<sup>†</sup>, Randall C. Johnson<sup>†</sup> and Owen R. Coté<sup>‡</sup><sup>†</sup> NOAA/ARL Field Research Division, Idaho Falls, ID<sup>‡</sup> U. S. Air Force Research Laboratory

## 1. INTRODUCTION

The need to better understand variations in optical turbulence is leading to the development of a new airborne temperature sensor. Optical turbulence, spatial fluctuations of index of refraction in the atmosphere, is the result of density fluctuations within the atmosphere. Within the atmospheric boundary-layer, such fluctuations often result from a combination of temperature and water vapor perturbations. Within the boundary layer phenomena can be studied using radars (Hardy and Ottertsten, 1969; Wilson et. al., 1994), hygrometers, and temperature measurements. Optical turbulence in higher regions of the atmosphere, near the top of the troposphere and in the lower stratosphere, is of much less significance to atmospheric science in general. But, it is of considerable importance in the design and implementation of lasers that will pass through these regions.

In the mid and upper troposphere and above, optical turbulence is driven almost exclusively by temperature fluctuations. The temperature fluctuations are actually the result of velocity perturbations in the presence of potential temperature gradients (Kundu, 1990). Assuming Kolmogorov theory, the index of refraction structure constant ( $C_n^2$ ) may be computed directly from temperature measurements. Traditionally, optical turbulence measurements at high levels have been made by a balloon-borne instrument, the Thermosonde (Jumper and Beland, 2000). The Thermosonde measures directly the temperature difference across a 1 m horizontal distance. From this, a running RMS average is computed. The RMS average is for all practical purposes identical to the temperature structure constant ( $C_T^2$ ) which is in turn proportional to  $C_n^2$ . The Thermosonde is an instrument for producing vertical profiles of  $C_n^2$  but is of little use for investigating the horizontal extent of optical turbulence layers.

Aircraft provide a vehicle from which to measure horizontal variations of  $C_n^2$ . Layers initially identified through vertical ascents/descents can be further probed by flying repeated transects over large horizontal areas. A joint venture by the Air Force Research Laboratory, NOAA Air Resources Laboratory (ARL), and Airborne

Research Australia recently conducted several experiments in Australia, Japan and London to study optical turbulence in the upper troposphere using aircraft. The Australian Egrett II was instrumented with three NOAA/ARL-designed 'Best Aircraft Turbulence' (BAT) probes (Crawford and Dobosy, 1992) to obtain measurements of temperature and velocity fluctuations. The experiment proved successful in providing the necessary measurements in strong turbulence (Coté et. al., 2000) but also identified an inability to measure temperature with sufficient speed and resolution in cases of weaker turbulence. Thus, the need for a new temperature probe was identified.

In this paper we discuss a recent effort to address the shortcomings of current probes to measure temperature with sufficient speed and resolution. The probe is still in its early stages of development, although a proto-type has been constructed and flown in August, 2000. We report on these efforts and on data collected during these test flights. In addition, we compare measurements from this new probe to measurements from the BAT probe and the Warsaw University-designed Ultra-Fast Temperature (UFT) Probe (Haman et. al. 1997). The UFT and BAT probe were flown simultaneously with the new probe during the test flights.

## 2. PROBE DESIGN

Four primary factors controlled the design of the probe; robustness, measurement resolution, time response, and well-behaved recovery factor. Measurements from previous campaigns indicate that a temperature resolution of 0.01 C and a time constant of 0.02 s would be sufficient to dramatically improve our ability to obtain  $C_n^2$  estimates in regions of weak to moderate turbulence.

## 2.1 Theoretical Considerations

A temperature probe measures some fraction of the 'total' temperature. The total temperature includes the static free-stream temperature *plus* the temperature rise due to dynamic heating (the conversion of kinetic energy of the air into thermal energy) *plus* a temperature departure due to radiation effects. The temperature rise due to dynamic heating increases as a square of the

To achieve the high resolution necessary for this probe it is important to construct a design for which the recovery factor remains constant. Depending on the design, the interaction between the sensing element and the airflow may change slightly with variations in flow angle. Flying at  $100 \text{ m s}^{-1}$  results in a dynamic heating term of roughly  $5 \text{ C}$ . A  $1\%$  variation in  $f_r$  leads to  $0.05 \text{ C}$  measurement error in temperature.

A fine sensing element also requires protection from the elements. Dust, insects, and other small particles can easily damage the element. To this end, it was decided a housing would be designed to protect the element and electronics. The primary concern then becomes how the housing affects the measurement. The transfer of heat from the housing to the air stream that is sensed must remain negligible. Also, the recovery factor of the housing must be insensitive to the angle of attack (and sideslip) of the probe.

For this design, it is important that air flows through the chamber fast enough that there is no significant heat transfer not only from the walls

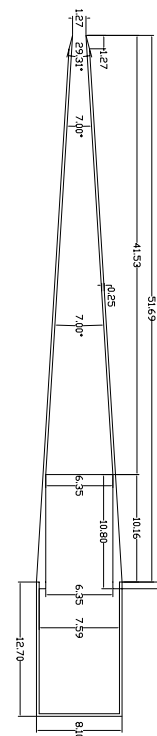


Fig 1. Housing for the newly designed airborne temperature probe. The cone points in the direction of flight. The sensor is located in the center of the chamber near the position where the expansion is complete. The electronics are contained in the rear portion, in the 12.7 cm long cylinder.

(across stream) but also up and down the flow direction. Too fast of a flow, on the other hand, would complicate the recovery of temperature. With the present design, the measured temperature can be described by:

$$T_m = T_s + f_{r1}(v_1^2/2c_p) + f_{r2}(v_2^2/2c_p), \quad (1)$$

where the subscript 1 refers to the housing and the subscript 2 refers to the element. The third term is small compared to the second ( $v_2^2 \ll v_1^2$ ) and we need only worry about the recovery of temperature due to the slowing of the air in the probe chamber.

## 2.4 Electronic Design

The sensing element is held in place by two struts from which it is electrically insulated. The reference junction is located well aft of the main junction, within the electronics section of the instrument (Fig. 1). This chamber is isolated from the main chamber of the probe using foam insulation. The reference junction is again Cu-Co and a micro-bead thermistor is attached to the junction with a large mass of epoxy. This design assures both the micro-bead and the junction are at the same temperature and that it responds slowly to temperature changes. The micro-bead thermistor supplies the reference temperature of the junction. The output from the thermocouple (referenced to junction) passes through two low noise amplifiers and an anti-aliasing filter before it is made available to the data system.

The raw thermocouple output is roughly  $40 \mu\text{V C}^{-1}$ . The front-end amplifier increases the signal to  $40 \text{ mV C}^{-1}$  while adding  $50 \mu\text{V}$  peak to peak noise. This noise corresponds to roughly  $0.001 \text{ C}$ . A second amplifier increases the signal to  $0.8 \text{ V C}^{-1}$ . The temperature drift in the amplifiers is  $<0.4 \mu\text{V C}^{-1}$ . The amplifiers are not insulated directly but are contained in the electronics section of the probe, isolated from the probe chamber.

## 3. TEST FLIGHTS

During a two week period from 03 August to 17 August, 2000, flight tests were conducted to evaluate the performance of the newly designed airborne temperature probe. The tests were based out of Idaho Falls, ID, utilizing the N3R LongEZ aircraft operated by personnel from NOAA/ARL Field Research Division.

In addition to the newly designed probe, two other temperature probes were mounted on the aircraft. A clear air version of the UFT (Haman et al., 2000) was operated by Dr. Kris Haman from Warsaw University. A BAT probe provided the 'center-piece' of the instrument suite. In addition to

temperature, the BAT probe also provides differential and static pressures, from which air speed and flow angle may be computed. This is necessary for the evaluation of recovery factors. To facilitate direct comparisons, the probes were spaced as closely as possible, in front of the nose of the aircraft.

The primary objectives of the flight tests were two fold. First, to compute and evaluate the recovery factors for all three temperature probes. It would be necessary to determine the sensitivity of the computed recovery factors to flow angles. Second, to evaluate the time response and resolution of each of the temperature probes. This would be accomplished both by direct comparison of temperature traces from each probe as well as looking at power spectra from each probe.

Nearly 20 hours were flown in 9 flights. Roughly half the hours were exhausted performing various maneuvers (pitch, yaw, acceleration/deceleration) to determine recovery factors and test the sensitivity of recovery factors to varying flow angles. The remaining flight hours focused on the collection of data during long horizontal passes and ascents/descents. Data collected in these patterns facilitate direct comparison between the probes. The following section discusses results from the preliminary analysis of data collected during the test flights.

## 4. RESULTS

### 4.1 Probe Recovery Factors

Recovery factors were computed by flying acceleration/deceleration runs at near constant altitude in regions of light turbulence. In doing so, it is assumed that the static temperature remains constant over the period of the maneuver. Fig. 2 shows a temperature trace from one such run on 09Aug. During this 400 second flight leg, air speed varies from  $40$  to  $75 \text{ m s}^{-1}$ . This corresponds to a dynamic heating of  $0.8$  to  $2.8 \text{ C}$ . The large variation in temperature is due to changes in airspeed and the corresponding dynamic heating.

From the Bernoulli equation, assuming an ideal gas, it may be shown that the velocity of a flow is given by:

$$V^2 = 2QR_dT/P_s, \quad (2)$$

where  $V^2$  is the velocity,  $Q$  is the dynamic pressure,  $T$  is the static temperature and  $P_s$  is the static pressure. Substituting this into equation (1), and assuming that the main contribution to dynamic heating comes from the housing results in:

$$T_m = T_s + (QR_d/c_p P_s)(f_r T_s). \quad (3)$$

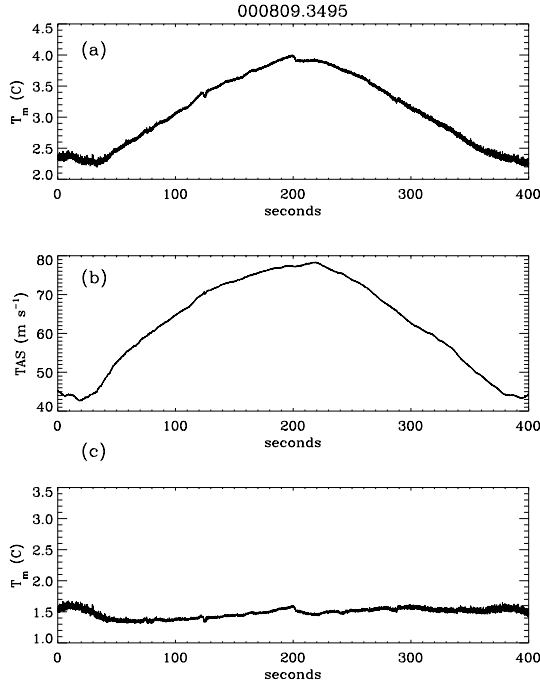


Fig 2. 400 second flight leg from 09Aug showing (a) measured temperature from the new probe (uncorrected for dynamic heating), (b) true air speed, and (c) measured temperature, corrected for dynamic heating.

The recovery factor may then be determined experimentally by plotting the measured temperature,  $T_m$ , as a function of the quantity  $(QR_d/c_p P_s)$ . This dimensionless quantity is related to the fraction of the total temperature that is due to dynamic heating. Fig. 3 shows plots of the measured temperature versus this quantity for the three probes. Applying a least squares linear fit results in an estimate of the static temperature from the intercept. The recovery factor is determined by dividing the slope by the intercept.

For both the new probe and the UFT, the data are well represented by a linear fit. Computed static temperatures are nearly equal (272.5 K). The calculated recovery factor for the new probe is 0.79, for the UFT it is 0.88. Both are within the expected range. Fig. 2c shows a plot of temperature from the new probe for the same period corrected for dynamic heating. Note that there is little variation related to maneuver.

Results from the BAT probe differ significantly (Fig. 3c). In this case, the data are nearly linear for higher speeds, but depart significantly from the linear model at lower airspeeds. The lower airspeeds correspond to larger attack angles. Faster airspeeds correspond to a near zero angle of attack. When the angle of attack becomes

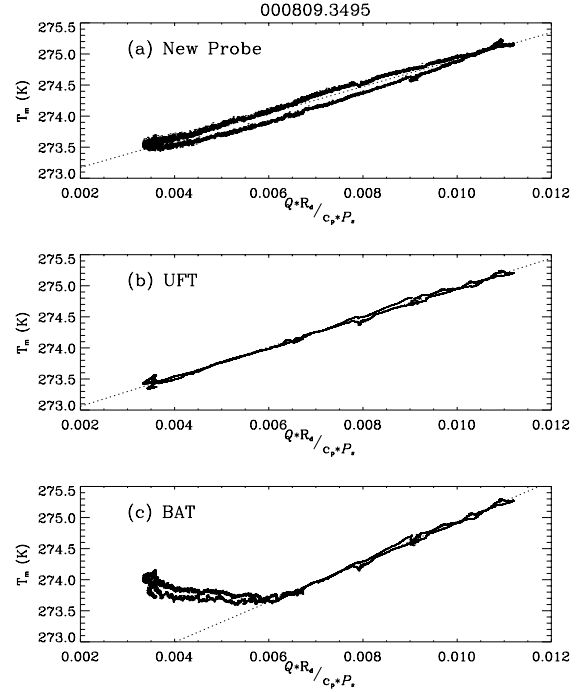


Fig 3. Measured temperature from the (a) new probe, (b) UFT, and (c) BAT probe plotted as a function of the dimensionless quantity,  $QR_d/c_p P_s$ , see text for explanation.

greater than roughly three degrees, the probe begins to fail to recover the temperature. This is likely due to the location of the sensing element in the BAT housing and the size of the port in which the micro-bead is located (see Appendix A).

#### 4.2 Time Response and Resolution

Fig. 4 shows a temperature trace from the new probe during a straight and level flight segment of roughly 700 s in duration. The data were collected at 3.7 km above mean sea level. Note the temperature scale, fluctuations are small over the entire leg. Fig. 4b shows a 10 s segment of this leg, from 280 to 290 seconds. In general, the data appear noisy, but only at a level of 0.05 C. It does appear that the probe responds quite fast to small temperature excursions. At 287.5 seconds, a small drop in temperature of roughly 0.15 degrees is measured by the probe. This occurs over a period of 0.1 seconds. Power spectra for the entire 700 s is shown in Fig. 4c. There appear three distinct regions. Slower than 1 Hz (spatial scales greater than 60 m) the spectrum has a -5/3 slope. From 1 to 10 Hz (60 cm to 60 m) the slope flattens out. Above 10 Hz (shorter than 60 cm) the spectrum once again has a slope of -5/3. The behavior is difficult to explain. The filter cutoff is at 30 Hz, so the roll-off is not due to anti-alias filtering.

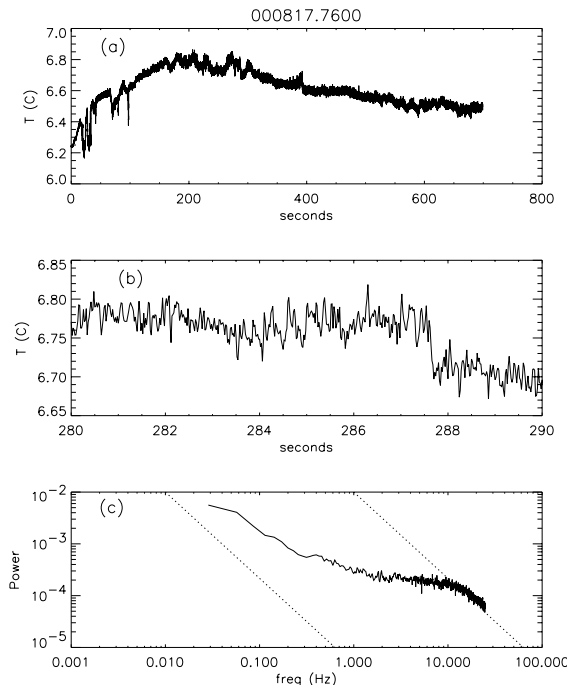


Fig 4. Temperature (a) from the new probe during a 700 s straight and level flight leg on 17Aug. (b) A 'blowup' showing a 10 s segment from 280 to 290 seconds from plot (a). Power spectrum (c) computed from the 700 s data segment.

Electronic noise would extend out to all higher frequencies and there would be no return to the  $-5/3$  slope beyond 10 Hz. At this time we are unable to offer explanation regarding the behavior of the spectra.

## 5. CONCLUDING REMARKS

In the preceding sections, a design for a new proto-type airborne temperature probe is presented. The primary goal is to produce a probe that is robust, insensitive to changes in flow direction (over what is typically encountered in flight), and responsive to temperature changes of 0.01 C at frequencies of 50 Hz. The design proved to be robust and has a constant recovery factor. Unfortunately, the noise level is greater than expected. The time response of the instrument is quite fast, but more data must be analyzed to quantify this statement.

More tests are warranted on this probe. Both ground tests and flight tests will be conducted in the coming months. Tests will likely focus on the effects of the housing. Based on the flight tests with the UFT, we feel the addition of a housing to this probe may be an over-complication of the problem.

## 6. APPENDIX A

The BAT Probe consists of a 15-cm diameter hemisphere mounted on the end of a tapered carbon-fiber cone (<http://www.noaa.inel.gov/frd/Capabilities/Bat/>). The housing contains nine holes from which three differential pressures and static pressure is measured. The center hole, the Design Stagnation Port (DSP) faces the flight direction of the aircraft. It is within this port that dynamic pressure is measured. The BAT temperature sensor (micro-bead) is also located within the DSP, directly in front of the pressure sensor (Fig. A1). Based on the size of the vent holes located behind the pressure sensor, the flow passes through the DSP at a speed of 20% of its free-stream value. The diameter of the DSP is 6.35 mm. This corresponds to about 6 degrees given the diameter of the housing. For attack (and sideslip) angles from -3 to 3 degrees, the stagnation point is located in front of the DSP. This is not true for larger angles.

## 7. ACKNOWLEDGEMENTS

The authors thank Dr. Kris Haman of Warsaw University for providing and operating the UFT. Dr. Ron Dobosy of NOAA/ARL/ATDD helped in the initial analysis of the data. This work was funded under AFSAEC MIPR# NAFSAC99710497 and ARFL contract# RVSHA000686071.

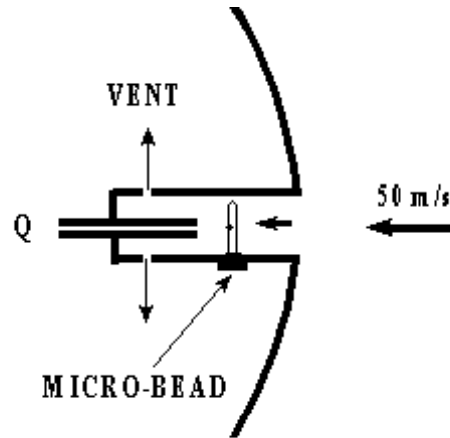
## 8. REFERENCES

- Coté, O. R., J. M. Hacker, T. L. Crawford, and R. J. Dobosy, 2000: Clear air turbulence and refractive turbulence in upper troposphere and lower stratosphere. *Ninth Conf. On Aviation, Range, and Aerospace Meteorol.*
- Crawford, T. L., and R. J. Dobosy, 1992: A sensitive fast-response probe to measure turbulence and heat flux from any airplane. *B-L Meteorol.*, **59**, 257-278.
- Haman, K. E., A. Makulski, S. P. Malinowski, and R. Busen, 1997: A new ultrafast thermometer for airborne measurements in clouds. *J. Atmos. Sci.*, **14**, 217-227.
- Haman, K. E., S. P. Malinowski, A. Makulski, B. D. Stroe, R. Busen, A. Stefkó, and H. Siebert, 2000: A family of ultrafast aircraft thermometers for warm and supercooled clouds and various types of aircraft. *13<sup>th</sup> International Conf. On Clouds and Precip.*, Reno, NV, Aug. 14-18.
- Hardy, K. R., and H. Ottertsten, 1969: Radar investigations of convective patterns in the clear atmosphere. *J. Atmos. Sci.*, **26**, 666-672.

Jumper, G. Y., and R. R. Beland, 2000: Progress in the understanding and modeling of atmospheric optical turbulence. *31<sup>st</sup> AIAA Plasmadynamics and Lasers Conf.*, Am. Institute Aeronautics and Astronautics, Reston, VA.

Kundu, P. K., 1990: *Fluid Mechanics*. Academic Press, Inc., New York, NY, p 20.

Wilson, J. W., T. M. Weckwerth, J. Vivekanandan, R. M. Wakimoto, and R. W. Russell, 1994: Boundary layer clear-air radar echoes: Origin of echoes and accuracy of derived winds. *J. Atmos. Ocean. Tech.*, **11**, 1184-1206.



Stagnation Port Cross-Section with  $\mu$ -bead

Fig A1. A Cross-section showing the location of the micro-bead within the BAT probe DSP. The drawing is not to scale.